22nd International Conference on Sustainable Energy Technologies
Kuala Lumpur, Malaysia, 13 to 15 August 2026 · ISBN 978-1-995850-00-9 · ISSN 2978-4387

CONFERENCE PAPER · ENERGY STORAGE & CONVERSION

Decarbonization of Residential Buildings Using Low-Charge R290 Heat Pumps: Experimental and Numerical Approach

Mohammad Salman[1], Sun-Ik Na[1], Bongsu Choi[1], Bong Seong Oh[1], Ho-Sang Ra[1], Beomjoon Lee[1], Junhyun Cho[1], Gilbong Lee[1]*

[1] Korea Institute of Energy Research, Daejeon, Republic of Korea

RECEIVED 7 May 2026 · REVISED 6 June 2026 · ACCEPTED 16 June 2026
PRESENTED 13 to 15 August 2026 · PUBLISHED 23 November 2026

ABSTRACT

Decarbonization of residential buildings is a critical strategy for mitigating greenhouse gas emissions, with heat pump systems emerging as a viable alternative to conventional fossil-fuel-based heating technologies. Among natural refrigerants, R290 (propane) is particularly promising due to its negligible global warming potential and favourable thermophysical properties. However, its flammability imposes strict constraints on allowable refrigerant charge, necessitating the development of low-charge system designs for safe residential applications. This study presents a combined experimental and numerical investigation of refrigerant charge reduction in a water-to-water R290 heat pump system for residential use. The effects of heat exchanger geometry and compressor modulation on system performance are systematically analysed. A numerical model is developed to simulate system performance and is validated against experimental measurements. The specific charge (g/kW) is adopted as a key performance metric to quantify charge efficiency relative to heating capacity. The results demonstrate that optimized system design and operating conditions can significantly reduce refrigerant charge while maintaining stable thermal performance. A minimum specific charge of 24.12 g/kW is achieved using the asymmetric heat exchanger configuration in combination with variable-speed compressor operation, without compromising the system efficiency. Furthermore, the findings suggest that low-charge R290 heat pump systems have strong potential for integration into advanced thermal energy storage technologies, such as Carnot Battery systems, where efficient heat transfer and minimized refrigerant inventory are critical for system scalability and safety. This highlights the broader applicability of the proposed approach beyond residential heating.

KEYWORDS R290 heat pump, Specific charge (g/kW), Charge minimization, Decarbonization

1. Introduction

The building sector is responsible for approximately one-third of global final energy consumption and carbon dioxide emissions, with residential space heating and domestic hot water accounting for a substantial proportion of building energy demand. Consequently, decarbonizing residential heating has become a key objective in achieving global climate neutrality and energy sustainability. Among the available technologies, electrically driven heat pump systems have emerged as one of the most effective solutions because they can deliver several units of thermal energy for every unit of electrical energy consumed. As electricity generation increasingly shifts towards renewable energy sources, heat pumps are expected to replace conventional fossil-fuel-based heating systems and become the dominant residential heating technology in future low-carbon energy systems (International Energy Agency (IEA) 2024; Hepbasli and Kalinci 2009).

* Corresponding author. Email address: giblee@kier.re.kr (Gilbong Lee)

© 2026 The Author(s).
Published by Caravel Press.

doi.org/10.65582/set.2026.010

While the energy efficiency of heat pumps has improved considerably over the past two decades, their overall environmental performance is also strongly influenced by the refrigerant employed. Conventional hydrofluorocarbons (HFCs), such as R410A and R134a, possess relatively high global warming potentials (GWPs) and are being progressively phased down under the Kigali Amendment to the Montreal Protocol and regional F-gas regulations. Consequently, considerable research has focused on environmentally benign refrigerants with low climate impact. Among the available alternatives, propane (R290) has received significant attention owing to its negligible GWP of approximately 3, zero ozone depletion potential (ODP), excellent thermodynamic properties, high latent heat of vaporization, favourable heat-transfer characteristics, and relatively low pressure losses. Numerous investigations have demonstrated that R290 can achieve heating performance comparable to or better than conventional HFC refrigerants while substantially reducing the environmental footprint of residential heat pump systems (Palm 2008; Elatar *et al.* 2025; Tang *et al.* 2018).

Despite these advantages, the commercial deployment of R290 heat pumps remains primarily constrained by its A3 flammability classification. Unlike conventional refrigerants, the maximum allowable refrigerant charge in residential equipment is restricted by international safety standards, including IEC 60335-2-40 (International Electrotechnical Commission (IEC) 2022). These safety requirements have fundamentally changed the design philosophy of residential heat pumps. Instead of maximizing system efficiency alone, modern heat pump systems must simultaneously satisfy multiple and often conflicting objectives, including thermal performance, refrigerant safety, environmental sustainability, compactness, manufacturing cost, and regulatory compliance. Consequently, refrigerant charge has evolved from being merely an operational parameter to a critical system design variable that directly determines the feasibility of residential R290 heat pumps.

From an engineering perspective, refrigerant charge is governed by the combined interaction of component internal volume, refrigerant distribution, operating conditions, compressor characteristics, oil circulation, and piping configuration. Therefore, reducing the refrigerant charge cannot be achieved simply by decreasing the mass of refrigerant charged into the system. Excessive charge reduction may result in insufficient evaporator wetting, incomplete condenser utilization, unstable refrigerant circulation, elevated compressor discharge temperatures, and deterioration of heating capacity and coefficient of performance (COP). Conversely, excessive refrigerant inventory increases inactive refrigerant accumulation within system components, reduces charge efficiency, and compromises compliance with safety regulations. Therefore, the engineering challenge is to optimize refrigerant distribution throughout the system while maintaining sufficient heat transfer and stable compressor operation under varying operating conditions.

To address this challenge, numerous charge reduction strategies have been investigated, including compact system layouts, reduced piping lengths, microchannel heat exchangers, compact plate heat exchangers, electronic expansion valve optimization, and variable-speed compressor operation. Among these approaches, plate heat exchangers (PHEs) are particularly attractive because their compact geometry and relatively small internal volume enable substantial reductions in refrigerant inventory without significantly sacrificing heat transfer performance. Furthermore, asymmetric plate heat exchangers offer additional opportunities to minimize internal refrigerant volume while maintaining favourable thermal characteristics. Similarly, variable-speed compressors provide operational flexibility by adjusting refrigerant circulation according to thermal demand, thereby improving refrigerant utilization over a wide range of operating conditions. Although these approaches have individually demonstrated promising results, their combined influence on refrigerant charge reduction has not yet been comprehensively investigated, particularly for residential water-to-water R290 heat pump systems.

Previous studies have primarily focused on improving heating capacity, coefficient of performance, and component efficiency, whereas refrigerant charge has frequently been considered a secondary performance parameter. Consequently, relatively limited attention has been devoted to

establishing systematic relationships between heat exchanger geometry, compressor modulation, refrigerant distribution, and overall refrigerant inventory. Moreover, refrigerant charge is generally reported as an absolute mass, making meaningful comparison between systems with different heating capacities difficult. The concept of specific charge (g/kW) provides a more representative performance indicator by relating refrigerant inventory directly to useful heating capacity, thereby enabling quantitative evaluation of charge utilization efficiency across different system configurations.

Motivated by these research needs, this study presents a combined experimental and numerical investigation of refrigerant charge reduction in a residential water-to-water R290 heat pump employing different plate heat exchanger configurations and variable-speed compressor operation. A numerical model was developed and validated using experimental measurements to investigate the influence of heat exchanger geometry and compressor modulation on refrigerant charge, heating capacity, COP, and specific charge. The principal objective was to identify operating conditions and component configurations capable of minimizing refrigerant inventory while maintaining stable thermal performance. The findings provide practical engineering guidelines for the development of compact, efficient, and safe low-charge R290 heat pump systems for future residential heating applications and advanced thermal energy storage technologies.

2. Methodology

2.1. Research strategy and experimental facility

The research begins with component/configuration screening, proceeds to baseline experiments, develops and validates a cycle model, applies numerical optimization, and then tests a compactified system. This sequence separates the influence of heat-exchanger geometry from the later influence of total system refrigerant-side volume and compressor operating conditions. The experimental facility is a closed-loop W2W vapor-compression heat-pump system using R290 as the working fluid. The refrigerant loop consists of a compressor, condenser, electronic expansion valve (EEV) and evaporator. Water-side circuits supply the heat source and heat sink, and the facility includes temperature/pressure measurement and data-acquisition equipment for steady-state evaluation. The system schematic is shown in Figure 1. The equipment information for the experimental facility is available in Table 1.

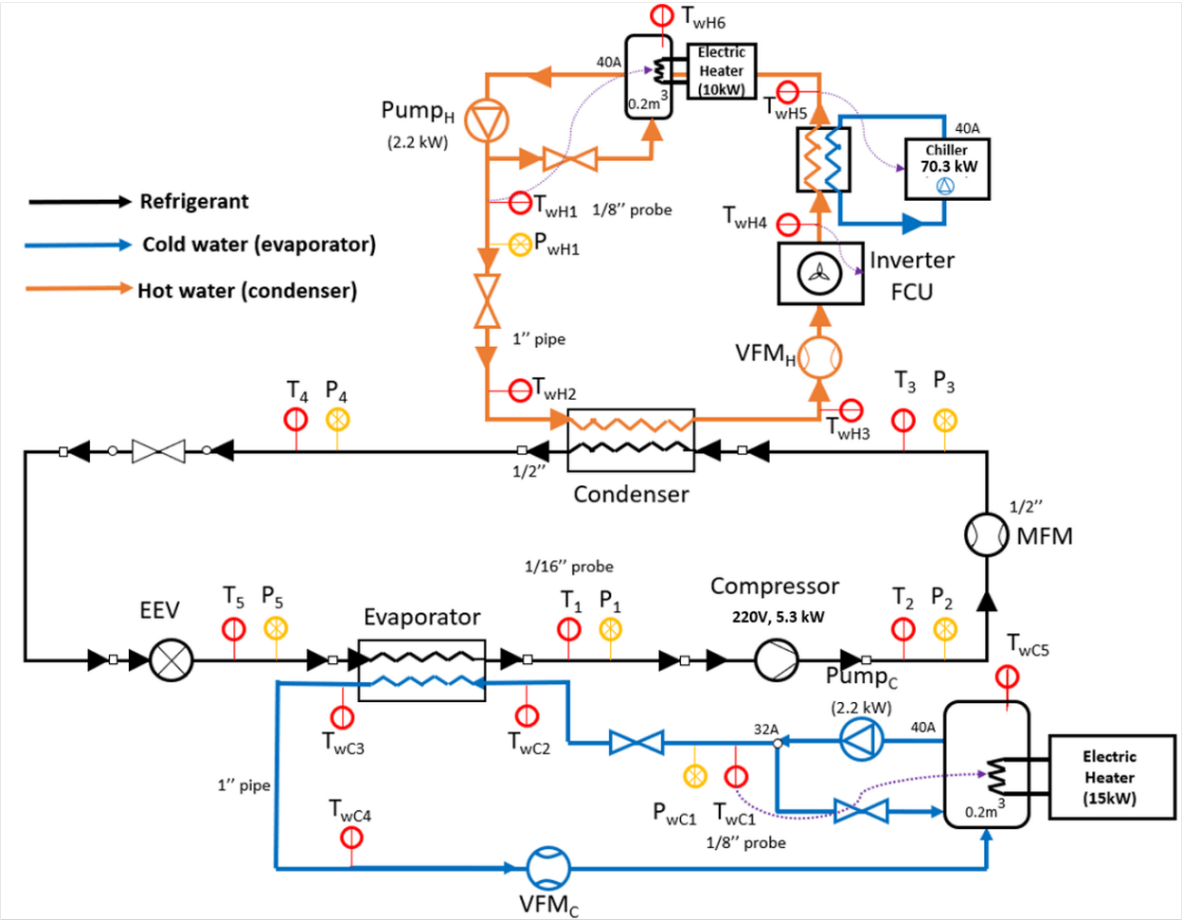

Figure 1. Schematic of the experimental W2W R290 heat-pump facility.

Table 1. Principal equipment information available for the experimental facility.

Component	Specification
Compressor	Hermetic rotary; 30 cc/rev displacement; 4-pole motor; 16.45 kg; operating range 15–110 rps
Digital power meter	Yokogawa WT333E; 15–600 V; 2.5 mA–20 A
Electronic expansion valve	Sanhua; 1–13.3 USRT capacity; pulse-controlled, high-precision EEV
Working fluid	R290 (propane)

2.2. Heat-exchanger configurations and baseline tests

Three PHE configurations were evaluated: a symmetric and two asymmetric configurations, denoted Asymmetric HX1 and Asymmetric HX2. The description of the heat exchangers used is mentioned in Table 2. The comparison was performed at three source/sink conditions: W5W45, W10W45, and W10W50. Baseline compressor speed was 4800 rpm, and the superheat condition shown in the source results was 10 K. The purpose of this stage was to identify the heat exchanger that simultaneously provides high COP and low specific charge.

Table 2. Heat exchangers used.

	Geometry	Height[mm]	Number of Plates	Hold-up volume [dm³]
Condenser (HX)	Symmetric	526	20	1
	Asymmetric HX1	526	18	0.8
	Asymmetric HX2	376	24	0.48
Evaporator (HX)	Symmetric	526	18	0.89
	Asymmetric HX1	526	18	0.8
	Asymmetric HX2	376	18	0.57

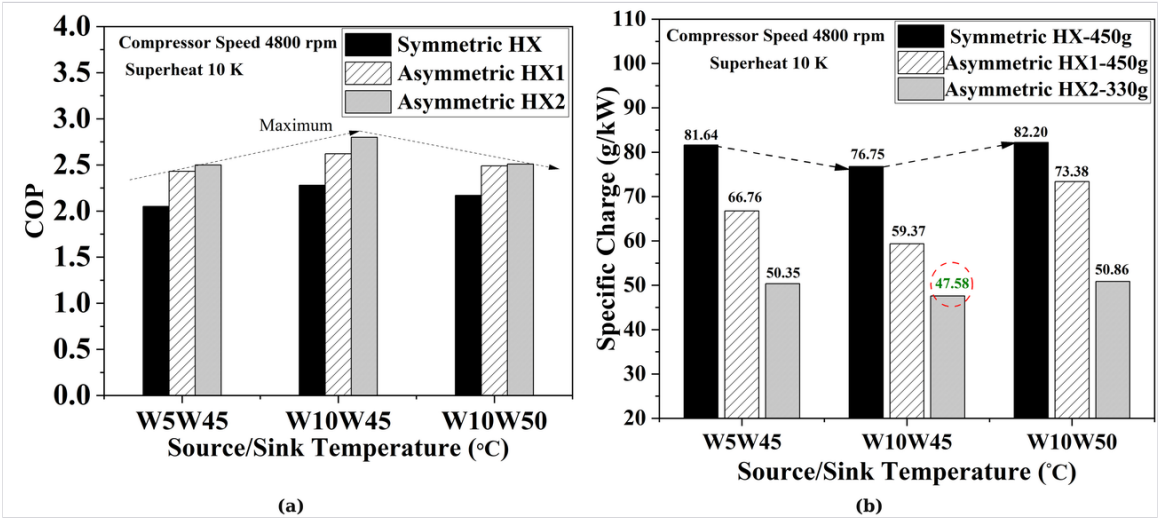

Figure 2. (a) Baseline COP comparison of symmetric and asymmetric heat exchangers at 4800 rpm and 10 K superheat, (b) Baseline specific charge comparison of the three heat-exchanger configurations.

Figure 2(a) compares the COP of the symmetric HX, asymmetric HX1, and asymmetric HX2 under different source and sink temperature conditions. Raising the source temperature from 5 °C to 10 °C resulted in an increase in COP for all three heat-exchanger configurations. This behaviour was attributed to the higher evaporation temperature associated with the warmer heat source, which reduced the required compression ratio and consequently decreased the compressor work. The corresponding COP improvement was approximately 9 % for the symmetric HX, 5 % for asymmetric HX1, and 7 % for asymmetric HX2. Despite the different rates of improvement, asymmetric HX2 maintained the highest COP throughout the investigated conditions, indicating its favourable thermal performance among the tested configurations. In contrast, increasing the sink outlet temperature from 45 °C to 50 °C resulted in a reduction in COP for all configurations. The higher sink temperature required a higher condensing temperature and pressure, which increased the compressor power requirement and consequently reduced the overall cycle efficiency. The COP reduction was approximately 6 % for the symmetric HX and 6.5 % for asymmetric HX2, with the remaining configuration showing a similar response. Nevertheless, asymmetric HX2 continued to provide the highest COP, demonstrating that its performance advantage was maintained even when the operating temperature conditions were varied. Overall, the results indicated that source temperature had a more favourable influence on COP, whereas an increase in sink temperature imposed a clear efficiency penalty across all three heat-exchanger configurations.

Figure 2(b) compares the specific charge (g/kW) of the symmetric HX, asymmetric HX1, and asymmetric HX2 at W5W45, W10W45, and W10W50, with the superheat maintained at 10 K. The refrigerant charges were 450 g for the symmetric HX and asymmetric HX1, while asymmetric HX2 operated at 330 g. The symmetric HX showed the highest specific charge, ranging from 76.75 to 82.20

g/kW, whereas asymmetric HX1 exhibited lower values of 59.37–73.38 g/kW. The reduction was attributed to the more compact asymmetric geometry and improved refrigerant distribution. Among the three configurations, asymmetric HX2 achieved the lowest RCC under all operating conditions, with values of 50.35 g/kW at W5W45, 47.58 g/kW at W10W45, and 50.86 g/kW at W10W50. The minimum value occurred at W10W45, indicating the most favourable combination of source and sink temperatures for charge utilisation. The relatively small variation in RCC for asymmetric HX2 also indicated consistent performance over the tested temperature range. Overall, the results demonstrated that the asymmetric HX2 configuration achieved substantially lower refrigerant charge per unit heating capacity while maintaining stable performance, making it the most favourable configuration for the subsequent low-charge optimisation.

2.3. Performance indicators

Heating capacity is obtained from the water-side energy balance,

$$\dot{Q}_h = \dot{m}_w c_{p,w}(T_{w,out} - T_{w,in}) \tag{1}$$

where $\dot{m}_w$ is the water mass flow rate, $c_{p,w}$ is the specific heat capacity of water, and T is the temperature.

System COP is evaluated from the useful heating capacity and measured electrical input,

$$COP = \frac{\dot{Q}_h}{\dot{W}_{comp}} \tag{2}$$

Where $\dot{W}_{comp}$ is the compressor power input and can be obtained from direct measurements using a power meter.

The principal charge metric is the specific charge,

$$\text{Specific charge} = \frac{m_r\,(\text{g})}{\dot{Q}_h\,(\text{kW})} \tag{3}$$

Where m_r is the total refrigerant charge.

This metric was selected because it allows charge efficiency to be compared while accounting for differences in useful heating output. It also directly supports the low-charge objective of the present study.

2.4. Numerical model and optimization

A vapor-compression cycle model was developed using the measured system configuration. The computational workflow consisted of experimental data input and steady-state screening, thermodynamic-property calculation using Python and CoolProp, compressor modelling, condenser/evaporator heat-transfer and refrigerant-charge calculations, and numerical optimization. The optimization procedure used the Trust Region Reflective method to vary operating conditions and identify a low-charge region. The model was not used to replace experiments; rather, it was used to reduce the experimental search space and identify promising charge/operating combinations. Validation was performed by comparing model predictions of specific charge against the corresponding experimental values (Figure 3). The parity plot uses ±10% and ±20% deviation bands. The majority of calculated points are located within the ±20% region, indicating that the model reproduces the overall charge-performance relationship sufficiently for optimization screening.

Because detailed point-by-point uncertainty statistics were not included in the source draft, the present paper reports the graphical validation rather than introducing unverified error statistics.

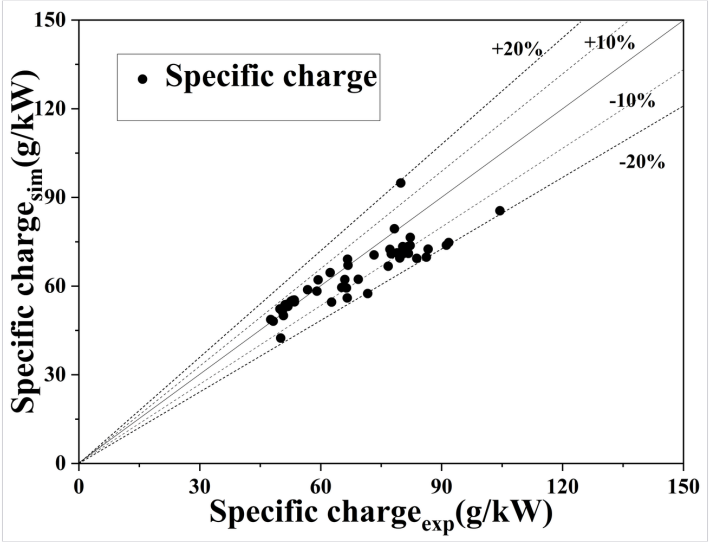

Figure 3. Comparison of simulated and experimental specific charge with ±10% and ±20% deviation bands.

2.5. Compact-system redesign

Following the baseline and numerical optimization stages, the system was redesigned to reduce refrigerant-side internal volume and non-useful refrigerant inventory. The redesign included shorter refrigerant piping, removal of the mass-flow meter from the refrigerant circuit, reduction of oil charge, and coordinated selection of heat exchanger, compressor, and operating conditions. The staged compactification approach is summarized by the source results as (Figure 4): Method 1—mass-flow-meter removal; Method 2—Method 1 plus 50% reduction in piping length; Method 3—Method 1 + 2 plus 50% reduction in receiver-side volume; Method 4—Method 1 + 2 + 3 plus increased compressor displacement; and Method 5—Method 1 + 2 + 3 + 4 plus optimized superheat.

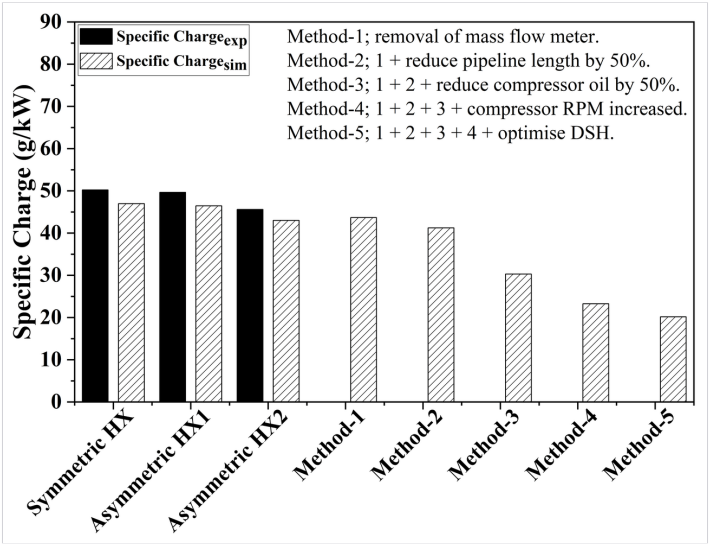

Figure 4. Effect of staged compactification methods (simulated results) on specific charge.

3. Results and discussion

3.1. Selection of the favourable heat exchanger

The baseline experimental stage shows that heat-exchanger geometry has a strong influence on both COP and specific charge (Figure 2). At 4800 rpm and 10 K superheat, the symmetric PHE produced the

highest baseline specific charge for all three source/sink conditions, while Asymmetric HX2 consistently produced the lowest. At W10W45, for example, the measured specific charges were 76.75 g/kW for the symmetric HX, 59.37 g/kW for Asymmetric HX1, and 47.58 g/kW for Asymmetric HX2. Thus, HX2 reduced specific charge by approximately 38% relative to the symmetric configuration under the same condition. This trend is consistent with earlier low-charge propane heat-pump research, where compact heat exchangers were identified as an effective means of reducing refrigerant inventory without necessarily sacrificing COP (Fernando *et al.* 2004; Sureddi *et al.* 2025). More recent R290 plate-heat-exchanger studies also show that the thermohydraulic behaviour of propane can support high heat-transfer performance in compact geometries when operating conditions are appropriately selected (Salman *et al.* 2023).

The same trend was observed at W5W45 and W10W50. The respective specific charge values for HX2 were 50.35 and 50.86 g/kW, compared with 81.64 and 82.20 g/kW for the symmetric heat exchanger. The consistency of the trend across the three operating conditions indicates that the advantage of HX2 is not limited to a single source/sink temperature combination. The result supports the central design premise that reducing refrigerant-side internal volume while retaining adequate heat-transfer area can improve charge efficiency. This interpretation is supported by Bani Issa *et al.* (2025), who identified heat-exchanger compactness and charge minimization as important design routes for residential R290 systems. The COP results provide an important qualification. The lower charge of HX2 was not obtained by sacrificing thermal performance. At W10W45, HX2 produced the highest COP of the three configurations, approximately 2.8 under the reported test condition, whereas the symmetric configuration was approximately 2.2. Similar relative behavior was observed at W5W45 and W10W50. The combined improvement in COP and specific charge makes HX2 the favorable configuration for subsequent charge optimization. This is particularly important because a low refrigerant mass by itself is not sufficient if the resulting heating capacity or efficiency is substantially degraded. Nawaz *et al.* (2017) similarly reported that R290 can provide competitive heat-pump performance while offering a lower refrigerant inventory than conventional R134a configurations, although the optimum system design remains dependent on component matching and operating conditions.

The minimum baseline value of 47.58 g/kW was obtained with Asymmetric HX2 at W10W45 and 330 g of R290. This value was adopted as the quantitative baseline against which the later compact-system improvement was evaluated. The result also illustrates why absolute charge alone is not an adequate comparison metric. A charge of several hundred grams can appear large or small depending on the heating capacity delivered by the system; normalizing by $\dot{Q}_h$ exposes the effectiveness of the refrigerant inventory. This type of charge-performance interpretation is consistent with the generalized analysis of Mehrabi and Yuill (2017), which showed that refrigerant-charge deviations affect multiple normalized heat-pump performance indicators and that the magnitude of the effect depends on system architecture and operating condition. The literature supports this interpretation. Liu *et al.* (2018) showed experimentally that R290 charge and superheat interact with expansion-device behaviour, and that electronic expansion control can help maintain performance at reduced charge. Nawaz *et al.* (2017) also demonstrated through a calibrated heat-pump model that R290 can achieve comparable residential water-heating performance with reduced refrigerant inventory. The present results extend these observations to a W2W configuration by explicitly linking heat-exchanger geometry and system compactification to specific charge. The use of a normalized metric is particularly useful because it separates the benefit of reducing inventory from the effect of simply changing system capacity.

3.2. Model validation and numerical optimization

The numerical workflow was used after the component-screening experiments to explore combinations that would be expensive to test exhaustively. Figure 3 compares simulated and experimental specific charge. The data cluster around the parity line and the majority of points lie

within ±20%, with a substantial number closer to the ±10% band. The model therefore captures the principal dependence of specific charge on the operating variables sufficiently well for a screening-level optimization. This modelling philosophy is consistent with recent work showing that finite-volume heat-exchanger models can be used to evaluate refrigerant charge and heat-transfer behaviour in R290 systems, provided that the underlying heat-transfer correlations are appropriately selected (Jung *et al.* 2026). Trust Region Reflective optimization predicted a low-charge operating region of approximately 120–170 g and a specific charge of approximately 20 g/kW (Figure 4). This prediction should be interpreted as a model-based target rather than an experimentally demonstrated minimum. In particular, operation at the lowest predicted charge may impose additional constraints associated with discharge temperature, compressor work, evaporator utilization and control stability. This distinction between a mathematical optimum and a practical operating point is important in variable-capacity systems. Kim and Braun (2015) demonstrated that variable-speed compressor systems require charge-estimation approaches that account for compressor speed and refrigerant-state variables, while Liang *et al.* (2026) recently showed that charge estimation in variable-speed heat pumps can be improved using physically informed feature selection. These studies support the present strategy of using the model to narrow the experimental search space rather than treating the numerical optimum as an automatically achievable operating point.

3.3. Effect of refrigerant charge and superheat

After selecting Asymmetric HX2 (from baseline results), charge sensitivity was evaluated under W10W45 for superheat settings of 10, 15, and 20 K. Figure 5 shows that specific charge exhibits a broad minimum rather than decreasing monotonically with decreasing refrigerant mass. At the lower-charge end, the specific charge rises because the reduction in refrigerant mass is accompanied by a reduction in useful heating performance. At higher charges, additional refrigerant does not proportionally increase useful heating capacity and therefore the g/kW metric rises again. The resulting U-shaped behavior identifies an operating region rather than a single universally optimal charge. Similar non-linear charge-performance behaviour has been reported for vapor-compression heat pumps and air-conditioning systems (Mehrabi and Yuill 2017; Liu *et al.* 2018).

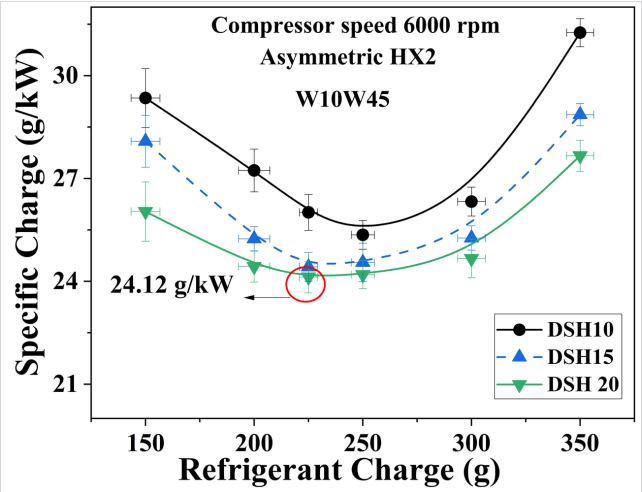

Figure 5. Specific charge versus total R290 charge for Asymmetric HX2 at W10W45.

The minimum experimentally demonstrated value in the compact-system tests was 24.12 g/kW at 225 g charge and the reported superheat/operating condition. Importantly, 225 g was selected as a practical operating point rather than simply choosing the lowest tested charge. The source results indicate that this condition maintained a substantially lower discharge temperature than the lowest-charge condition. This demonstrates a central engineering trade-off: the lowest refrigerant inventory

is not necessarily the best operating point when compressor thermal limits and stable system operation are included in the objective. This behavior is physically consistent with the concept of an optimum charge in variable-capacity systems and with experimental observations for R290 systems, where superheat and expansion-device operation influence the response to charge variation (Liu *et al.* 2018). It is also consistent with the low-charge propane heat-pump experiments of Fernando *et al.* (2004), who demonstrated that approximately 200 g of R290 could operate a 5 kW water-to-water heat pump without a COP penalty relative to a conventional design. More recent residential field testing has likewise shown that substantial R290 charge reduction can be achieved while retaining useful system performance (Elatar *et al.* 2025).

3.4. Compressor-speed effect and practical operating window

Compressor modulation provides an additional control variable for managing useful heating output at low refrigerant charge. Figure 6 shows the measured compressor work for Asymmetric HX2 at W10W45 for 150, 225, and 250 g charge. Compressor work increases with speed and also changes with charge. The 225 g case provides an intermediate operating condition between the lowest and higher charge cases, illustrating why compressor speed can be used to recover useful capacity without simply increasing the total refrigerant inventory. This interpretation agrees with variable-speed refrigerant-charge research, which shows that compressor speed changes the relationship between system states and charge-sensitive performance indicators (Kim and Braun 2015).

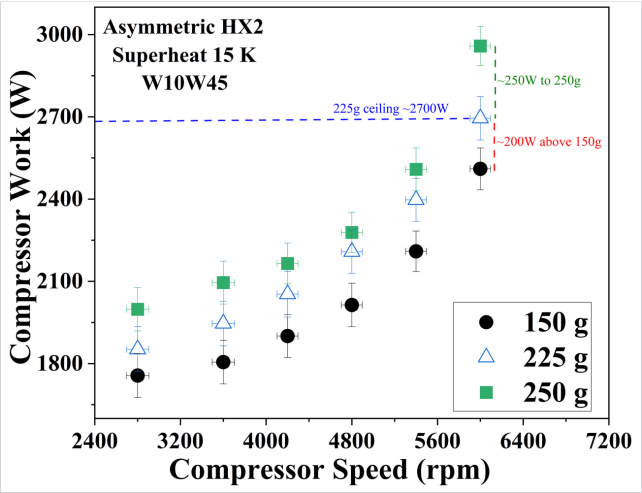

Figure 6. Compressor work versus compressor speed for Asymmetric HX2 at W10W45 for selected R290 charges.

The COP trend at 225 g and 15 K superheat further demonstrates the trade-off between output and compressor input. As shown in Figure 7, COP decreases from approximately 4.12 at the lower-speed condition to approximately 3.31 at the highest tested speed. Increasing speed therefore increases the available operating capacity but does not necessarily improve efficiency. The practical low-charge operating point should consequently be selected by considering heating demand, COP, discharge temperature and charge simultaneously. The importance of compressor and component matching is also evident in residential R290 heat-pump modelling, where compressor selection and operating conditions influence heating capacity, discharge temperature and total refrigerant charge (Nawaz *et al.* 2017; Ortega *et al.* 2024).

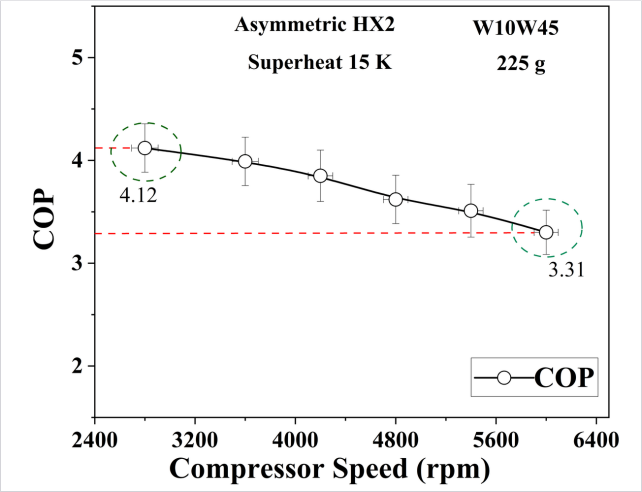

Figure 7. COP versus compressor speed for Asymmetric HX2 at W10W45, 225 g R290 and 15 K superheat.

4. Future plan

The current results establish a strong basis for the next stage of low-charge heat-pump development. The plan is organized around four complementary directions: miniaturized components, refrigerant-inventory quantification, online monitoring using on-board charge-quantification methods (Jounay *et al.* 2025), and AI-assisted optimization. Further validation is also required over a wider operating envelope. The current paper concentrates on the conditions represented in the available experiments, especially W10W45 and the 4800–6000 rpm range. Future work should examine seasonal source/sink variation, transient start-up and shutdown, repeated low-charge operation, leakage detection, and safety-oriented testing. These extensions are necessary before a laboratory low-charge design can be translated into a residential product. Finally, the low-charge architecture has potential beyond residential heating. Compact heat-transfer components and minimized refrigerant inventory are also attractive for advanced thermal-energy-storage systems such as Carnot Battery configurations, where compactness, efficient heat transfer, and safety can influence system scalability. This application will require a separate system-level assessment, but the present results provide a relevant low-charge heat-pump building block.

5. Conclusions

- Asymmetric HX2 was identified as the favorable heat-exchanger configuration among the tested symmetric and asymmetric designs. At W10W45, 4800 rpm, and 10 K superheat, HX2 achieved a baseline specific charge of 47.58 g/kW, compared with 76.75 g/kW for the symmetric configuration, while also providing the highest COP among the three configurations.
- The numerical model reproduced the experimental specific-charge trend with most validation points located within the ±20% deviation band.
- System compactification reduced refrigerant-side volume and unnecessary inventory through shorter piping, mass-flow-meter removal, reduced oil charge, and coordinated component/operating-condition optimization. The compact system achieved 24.12 g/kW experimentally, representing approximately 49% reduction from the 47.58 g/kW baseline.
- At 225 g R290, 24.12 g/kW was obtained while maintaining a substantially lower discharge temperature than the lowest-charge condition. This makes 225 g a practical operating point in the present experimental dataset, illustrating the need to balance minimum charge against compressor thermal limits and stable performance.
- The results demonstrate that low-charge R290 heat-pump development should be approached as a system-level optimization problem involving heat-exchanger geometry, refrigerant-side volume,

compressor modulation and operating control. The methodology provides a pathway toward safer and more compact residential heat pumps and can also support future applications requiring low refrigerant inventory, including advanced thermal-energy-storage systems.

Declarations

Author contributions. Mohammad Salman: Investigation, Formal analysis, Data curation, Writing (original draft), Visualization, Validation. Sun-Ik Na: Investigation, Formal analysis, Visualization, Validation, Data curation. Bongsu Choi: Writing (review and editing), Conceptualization, Methodology, Supervision, Project administration. Bong Seong Oh: Investigation, Data curation, Formal analysis. Ho-Sang Ra: Investigation, Data curation, Formal analysis. Beomjoon Lee: Conceptualization, Supervision, Project administration. Junhyun Cho: Funding acquisition, Conceptualization, Project administration, Supervision, Methodology. Gilbong Lee: Conceptualization, Funding acquisition, Project administration, Supervision, Methodology, Writing (review and editing).

Funding. This work was conducted under framework of the research and development program of the Korea Institute of Energy Research(C6-2410-37), and supported by the Korea Institute of Energy Technology Evaluation and Planning (KETEP) and the Ministry of Climate, Energy and Environment (Project No. RS-2025-25459261)

Awards. Korea Institute of Energy Research (C6-2410-37); and Korea Institute of Energy Technology Evaluation and Planning (RS-2025-25459261)

Conflicts of interest. The authors declare no competing interests.

Data availability. The data that support the findings of this study are available from the corresponding author upon reasonable request.

Generative AI. AI tools were used solely for language refinement and writing improvement

Acknowledgements. This work was conducted under framework of the research and development program of the Korea Institute of Energy Research(C6-2410-37), and supported by the Korea Institute of Energy Technology Evaluation and Planning (KETEP) and the Ministry of Climate, Energy and Environment (Project No. RS-2025-25459261)

References

Bani Issa, Abd Alrhman; Liang, Changkuan; Groll, Eckhard A.; Ziviani, Davide (2025) 'Residential heat pump and air conditioning systems with propane (R290) refrigerant: Technology review and future perspectives', *Applied Thermal Engineering*, 266, pp. 125560. Available at: https://doi.org/10.1016/j.applthermaleng.2025.125560

Elatar, Ahmed; Rendall, Joseph; Sun, Jian; Brechtl, Jamieson; Nawaz, Kashif (2025) 'Charge Reduction and Performance Analysis of a Heat Pump Water Heater Using R290 as a Refrigerant—A Field Study', *Energies*, 18(14), pp. 3661. Available at: https://doi.org/10.3390/en18143661

Fernando, Primal; Palm, Björn; Lundqvist, Per; Granryd, Eric (2004) 'Propane heat pump with low refrigerant charge: design and laboratory tests', *International Journal of Refrigeration*, 27(7), pp. 761-773. Available at: https://doi.org/10.1016/j.ijrefrig.2004.06.012

Hepbasli, Arif; Kalinci, Yildiz (2009) 'A review of heat pump water heating systems', *Renewable and Sustainable Energy Reviews*, 13(6-7), pp. 1211-1229. Available at: https://doi.org/10.1016/j.rser.2008.08.002

International Electrotechnical Commission (IEC) (2022) *IEC 60335-2-40: Household and similar electrical appliances—Safety—Part 2-40: Particular requirements for electrical heat pumps, air-conditioners and dehumidifiers*. Geneva: IEC.

International Energy Agency (IEA) (2024) *World Energy Outlook 2024*. Paris: IEA.

Jounay, Maëlle; Cauret, Odile; Teuillières, Cédric; Tran, Cong Toan (2025) 'A novel on-board method for quantifying refrigerant charge in residential heat pumps', *International Journal of Refrigeration*, 177, pp. 263-272. Available at: https://doi.org/10.1016/j.ijrefrig.2025.06.008

Jung, Minkyu; Song, Jiwon; Noh, Hyunkyu; Ku, Donik; Na, Sun-Ik; Lee, Gilbong; Kim, Minsung (2026) 'Validation of heat transfer coefficients in plate heat exchangers by estimating heat capacity and refrigerant charge of R290 heat pump

systems', *Journal of Mechanical Science and Technology*, 40(6), pp. 4753-4763. Available at: https://doi.org/10.1007/s12206-026-0549-6

Kim, Woohyun; Braun, James E. (2015) 'Extension of a virtual refrigerant charge sensor', *International Journal of Refrigeration*, 55, pp. 224-235. Available at: https://doi.org/10.1016/j.ijrefrig.2014.09.015

Liang, Chenjiyu; Guo, Fangzhou; Kim, Donghun; Hlanze, Philani; Cai, Jie (2026) 'Virtual refrigerant charge sensor for variable-speed heat pumps based on feature selection', *Applied Thermal Engineering*, 293, pp. 130290. Available at: https://doi.org/10.1016/j.applthermaleng.2026.130290

Liu, Cichong; Wang, Dandong; Sun, Ziyang; Chen, Liang; Shi, Junye; Chen, Jiangping (2018) 'Effects of charge on the performance of R290 air conditioner with different expansion devices', *Applied Thermal Engineering*, 140, pp. 498-504. Available at: https://doi.org/10.1016/j.applthermaleng.2018.05.077

Mehrabi, Mehdi; Yuill, David (2017) 'Generalized effects of refrigerant charge on normalized performance variables of air conditioners and heat pumps', *International Journal of Refrigeration*, 76, pp. 367-384. Available at: https://doi.org/10.1016/j.ijrefrig.2017.02.014

Nawaz, Kashif; Shen, Bo; Elatar, Ahmed; Baxter, Van; Abdelaziz, Omar (2017) 'R290 (propane) and R600a (isobutane) as natural refrigerants for residential heat pump water heaters', *Applied Thermal Engineering*, 127, pp. 870-883. Available at: https://doi.org/10.1016/j.applthermaleng.2017.08.080

Ortega, Ignacio; Sieres, Jaime; Cerdeira, Fernando; Álvarez, Estrella; Santos, José Manuel (2024) 'Research on the effect of the refrigerant charge in a variable capacity heat pump', *Science and Technology for the Built Environment*, 30(6), pp. 611-625. Available at: https://doi.org/10.1080/23744731.2024.2312798

Palm, Björn (2008) 'Hydrocarbons as refrigerants in small heat pump and refrigeration systems – A review', *International Journal of Refrigeration*, 31(4), pp. 552-563. Available at: https://doi.org/10.1016/j.ijrefrig.2007.11.016

Salman, Mohammad; Prabakaran, Rajendran; Kumar, Poongavanam Ganesh; Lee, Dongchan; Kim, Sung Chul (2023) 'Saturation flow boiling characteristics of R290 (propane) inside a brazed plate heat exchanger with offset strip fins', *International Journal of Heat and Mass Transfer*, 202, pp. 123778. Available at: https://doi.org/10.1016/j.ijheatmasstransfer.2022.123778

Sureddi, Roopesh Chowdary; Li, Liang; Wu, Hongwei; Giannetti, Niccolo; Saito, Kiyoshi; Rees, David (2025) 'A Review of Recent Advancements in Heat Pump Systems and Developments in Microchannel Heat Exchangers', *Machines*, 13(4), pp. 333. Available at: https://doi.org/10.3390/machines13040333

Tang, Weier; He, Guogeng; Zhou, Sai; Sun, Wei; Cai, Dehua; Mei, Kui (2018) 'The performance and risk assessment of R290 in a 13 kW air source heat pump', *Applied Thermal Engineering*, 144, pp. 392-402. Available at: https://doi.org/10.1016/j.applthermaleng.2018.08.070

HOW TO CITE THIS PAPER

Salman, M., Na, S., Choi, B., Oh, B. S., Ra, H., Lee, B., Cho, J. and Lee, G. (2026). Decarbonization of Residential Buildings Using Low-Charge R290 Heat Pumps: Experimental and Numerical Approach. In: *Proceedings of the 22nd International Conference on Sustainable Energy Technologies (SET2026)*, Kuala Lumpur, Malaysia, 13 to 15 August 2026. Caravel Press, pp. 121–133. ISBN 978-1-995850-00-9. ISSN 2978-4387. https://doi.org/10.65582/set.2026.010

COPYRIGHT AND LICENCE

© 2026 The Author(s). This is an open access paper distributed under the terms of the Creative Commons Attribution (CC BY 4.0) licence, which permits unrestricted use, distribution and reproduction in any medium, provided the original work is properly cited.

WSSET World Society of Sustainable Energy Technologies Organised by the World Society of Sustainable Energy Technologies. Published by Caravel Press.